The American Society of Mechanical Engineers

Reprinted From
HTD—Vol. 218, Micro/Macro Scale Phenomena in Solidification
Editors: C. Beckermann, L. A. Bertram, S. J. Pien, and R. E. Smelser
Book No. G00704 — 1992

AN ALTERNATIVE APPROACH TO MODELING THE GRAIN STRUCTURE OF CASTINGS

R. S. Steube and A. Hellawell
Department of Metallurgical and Materials Engineering
Michigan Technological University
Houghton, Michigan

ABSTRACT

During the past 25 years there has developed increasing interest in the possibility of being able to predict the overall solidification process in metal castings. This has obvious applications in the automation of foundry practice, improved quality control, and for innovative design. To model the entire process, numerically, involves the two major steps of (a) calculating the macroscopic heat flow and local temperature changes within the casting, and (b) matching this with a description of the pattern of microstructural development and latent heat evolution; the former has become routine but the latter remains less certain and open to discussion. The success of such models can be assessed by how accurately they predict the measured cooling curves and how closely they predict the corresponding microstructures, particularly the measured grain size. A majority of models have been applied to the near isothermal solidification of grey cast irons which develop a radial, duplex cell or grain structure; these involve semi-empirical models for heterogeneous nucleation on unspecified substrates of variable potency and population density. Considerable success has been achieved in fitting these modeling results to thermal analyses or to measured cell/grain counts, but not necessarily to both at once.

In the absence of specific heterogeneous nucleating agents, such as may be added deliberately as grain refiners, it has long been recognized that during casting, and perhaps with initial columnar grain growth, the bulk liquid typically contains a remarkably high population density of dendritic or other fragments of the base material, variously introduced. The presence of such crystal fragments may readily be observed in transparent analogue models based on aqueous or organic systems, i.e., by experimental rather than numerical modeling. It is suggested that an alternative, more physically realistic modeling route for equiaxed grain formation may be developed in terms of the production, distribution, survival and growth of these inherent crystal fragments. Some success has been achieved in predicting the equiaxed grain size of continuous steel castings, using such an alternative model, and the outline of an experimental and numerical modeling program is suggested.

Some of the points made in the text will be reinforced during presentation by the use of a video recording of fluid flow and crystal transport in aqueous analogue castings.

INTRODUCTION

There exists a vast literature reservoir covering all aspects of the subject of solidification from heat flow analyses, through the growth of single crystals, the macro- and microstructure of casting, and to those of welding, concerned with general and specific problems. These cover a wide range of cooling and freezing rates and scales of operation spread over six orders of magnitude or more (e.g., cooling rates up to 10^6 $K \cdot s^{-1}$, growth rates from < 1 $\mu m\ s^{-1}$ to 1 ms^{-1}, or scales from as low as 10 μm up to 10 m). Logically, over the previous three decades there has been an increasing number of attempts to assemble available data in order to model the overall, global aspect of solidification, as it might apply to a casting or liquid pool of given shape and size (during real foundry practice). If this can be done in a physically realistic and predictive manner, the effort has immense potential for

improved quality control, automation, and innovative design.

The first approach to modeling of this type was probably that pioneered by Oldfield (1960, 1966) for eutectic cast iron, using quite arbitrary and empirical expressions for nucleation and growth, and assuming a constant rate of heat removal. The attraction of cast irons, especially eutectic grey irons, is that they solidify with a pattern of nearly spherical eutectic colonies or cells, which are geometrically convenient to describe by an Avrami-type expression (1939) for nucleation, radial growth and ultimate impingement. This type of model has been developed and refined by many workers, notably Stefanescu et al (e.g., 1986, 1988) and Dantzig et al (e.g., 1992), with considerable success for simple shapes and specific compositions.

A broader general approach for nominally single phase and multiphase materials has also been set out by Rappaz and coworkers (e.g., 1989(a)(b)), and for all of these there are now available refined and adaptable codes for the macroscopic heat flow analysis in a wide range of configurations of alloys and molds (see, e.g., Engr. Foundation Proceedings, etc. 1980-1991). The macroscopic heat flow analyses are coupled with models for the evolution of the microstructure, and reiterative procedures can yield thermal analysis results, i.e., cooling curves to compare with those recorded and a description of the corresponding grain size(s) and scales of microsegregation, where relevant. It is this latter correlation which leaves some room for improvement and will be the focus of the present contribution.

In Oldfield's original approach and those which have followed, the development of the grain structure, the "equiaxed" structure, is assumed to follow by heterogeneous nucleation upon a family of unspecified substrates of variable potencies and population densities. This approach allows the grain size to be predicted in terms of the undercooling from the cooling rate, modified by growth and latent heat evolution, leading to recalescence. The treatment can be effected by relatively crude and simple assumptions or deal with the nucleation kinetics more rigorously. Such a heterogeneous model has some obvious justification when substrate particles are deliberately introduced into a melt to promote equiaxed grain formation, as is common practice in the grain refining of aluminum or magnesium based castings (Glasson et al 1967, Hellawell 1979), but even in these circumstances the identities and activities of the substrates themselves are complicated and ambiguous; see, e.g., Maxwell et al (1975). Even in isolated systems, as in small droplets, it has been demonstrated that an apparently unique substrate can exhibit a variety of activity at different undercoolings (Hoffmeyer et al, 1989). But in the more general and a majority of cases, including large scale ferrous operations, deliberate additions are not made to the melt, and yet equiaxed grain formation takes place in bulk liquid at small undercoolings.

As has been widely recognized for some time (e.g., Davies, 1973), the most effective source of such crystals is in the presence of fragments of the base material itself, inherently introduced during the casting operation and early stages of solidification. Three such source mechanisms may be identified:

(i) In the course of the initial chilling of liquid, making contact with the mold, either in a direct pouring operation or through a gating system, it is to be expected that many small crystals will nucleate and may be swept into the bulk liquid as the mold fills (or as material passes through it continuously). If the superheat is low, a significant fraction of these fragments may survive and give rise to an equiaxed grain structure with negligible columnar growth from the mold walls. This suggestion was made in the 1920's (Genders, 1926) and was revived for such a condition by Chalmers (1963), who termed it "big bang" nucleation.

(ii) A somewhat similar source, but operating in a longer time frame, is the upper liquid surface, particularly in castings where there is significant heat loss from that surface. Again, this was an early suggestion (Rosenhain, 1926), further invoked by Southin (1967) to explain observations in copper base castings.

Both (i) and (ii) have been suggested in a combined form to explain the origin of equiaxed grain formation in continuous steel castings (Lait et al, 1974 and Bommaraju, 1984).

(iii) At longer times ($\tilde{>}10^3$ s), as in larger and more slowly freezing ingots, when a significant (>10 mm) columnar mushy zone has developed, the initial dendritic framework itself can become a potential source of crystal fragments, as ripening and spheroidization cause side arms to separate from primary dendritic stalks. This type of behavior is accelerated in many casting situations as the velocity of the primary growth front decreases and as the temperature gradient across the mushy region decreases, causing local remelting. Such ripening and local remelting have been clearly demonstrated in transparent materials (e.g., Jackson et al, 1966 and Glicksman et al, 1968) and have been identified in metallic castings (Kattamis et al, 1965 & 1967, Biloni et al, 1968, Bower et al, 1967); quantitative measurements of ripening kinetics, such as those by Glicksman and Voorhees and coworkers (e.g., 1984,1985), are obviously most important in this context. It is also particularly relevant to this source mechanism that there be, simultaneously, fluid flow within and without the dendritic mushy zone in order to transport the crystal fragments to the bulk liquid and to distribute them so that survivors may grow into equiaxed grains. In the context of this

model, there arise the subsequent events, in that, as surviving crystals start to grow, they tend to sediment and eventually accumulate at some lower level in sufficient density to block further advance of the columnar front, thus affecting the columnar to equiaxed (C:E) transition in grain structure. This last aspect has received some attention recently (Jang et al, 1991) in attempts to model the C:E transition in the configuration of a continuous casting, but no attempt was made to link up the sequential steps of an overall mechanism.

AN ALTERNATIVE MODEL

It will be argued here that there is evidently an alternative approach to modeling grain size in a casting to that based on the existence of unidentified heterogeneous substrates, or, to put it another way, even in the presence of deliberate grain refining additions, there do exist, at all times, identifiable "nuclei" which are inherent in the operation. Moreover, the population density of such fragmentary embryos may be remarkably high, perhaps as great as 10^2 mm^{-3} in some situations (Sarazin et al, 1992). This suggests that an alternative modeling approach might then be devised which would consider these crystal fragments specifically and could be divided into four interdependent steps:

(a) The kinetics of fragment formation or "crystal multiplication." In the present discussion the principal, but not exclusive, concern will be with the last mechanism, (iii) above, i.e., originating in the mushy zone. Obviously, at low superheats, when an initial columnar mushy region does not develop, the alternative sources, (i) and (ii), may dominate. However, these would be very difficult to model indeed, except in an arbitrary, empirical format.

(b) The transport of fragments from the mushy zone (or elsewhere) into the bulk liquid. This may involve natural convection or forced stirring. A considerable body of observational evidence about natural, thermo-solutal patterns and transport rates is now available (e.g., 31), but quantitative analyses of forced stirring effects, e.g., electromagnetic, or of the effects of mold vibration are virtually nonexistent, although they are much used in practice.

(c) The survival rate (time) of crystal fragments in bulk liquid which lies above, but close to, the liquidus temperature, and

(d) The growth and sedimentation rates of fragments which survive long enough to enter a region below the liquidus temperature and, hence, the necessary sizes and population densities of these needed to block advance of the pre-existing columnar front; cf. ref. above.

In principle, the time and temperature dependence for each of these steps could be set up in a formal but arbitrary manner, each to interact in such a way as to yield a grain density with an associated cooling curve. But without a correct physical description, supported by experimental numerical data, the approach would have little better predictive capability than the heterogeneous model now employed, and would be more cumbersome to use. Therefore, it is pertinent to consider these steps in more detail, to assess the feasibility of obtaining good measured data and reaching physically realistic analyses at each stage. Thus:

(a) Ripening and Crystal Multiplication

As previously mentioned, earlier evidence of fragmentation within a dendritic mesh was demonstrated by Jackson et al (1966) using transparent organic analogues, and this was supported with similar observations by Glicksman et al (1968) and in metals by Flemings and others (1967-1968). This principal mechanism involves separation of dendrite side arms from the primary stalks, which is aided by solute rejection from the latter, causing a neck to develop at the base of a well-developed side arm, which, having a smaller radius of curvature than elsewhere, accelerates the ripening process locally, Fig. 1. The earlier observations were convincing demonstrations of such a mechanism for crystal multiplication, but were essentially qualitative. Subsequently, Glicksman and coworkers (1984) have carried out classical studies of high precision to follow ripening in solid-liquid dispersions of pure succinnonitrile (SCN), illustrating that this obeyed a $t^{-1/3}$ relation and was essentially stochastic. This work has continued (e.g., Glicksman and Marsh, Voorhees et al, 1985, 1992) with studies of ripening of dendritic arrays in the presence of solute. As one might expect, the same power law is obeyed but the process is retarded by the relatively lower diffusion coefficient for mass vs. heat transfer. Also to be emphasized is that the active size range for ripening is restricted at any time for radii of curvature, r, $0 < r < 1.5\ \bar{r}t$, where $\bar{r}t$ is the mean radius of curvature in the system at a time t. This means that, in a dendritic array of regular geometry, the coarser initial features of primary dendritic spines do not take part in the ripening process until after longer times, i.e., when they begin to fall below the $1.5\ \bar{r}t$ limit. Necessarily, this must also imply that the process is no longer entirely stochastic; in fact, quite the reverse, because the dendritic array is far from being random. The kinetics of fragmentation are a function of the initial dendritic morphology and of the solid fraction, therefore dependent on the alloy composition and growth/cooling rates. Some preliminary assessment of these factors has been made by both Glicksman and Voorhees

and by deliberate melting experiments on SCN dendrites by Sato, Kurz and Ikawa (1987). The prognosis for a quantitative analysis of this step seems to be good.

(b) Particle Transport

The concern here is with how dendrite particles escape from the mushy region and are subsequently distributed throughout the bulk liquid. Without forced stirring or agitation, natural thermo-solutal convection is clearly one, if not the principal, process involved in this transport. During solidification, thermal and solutal density changes are inevitable within a system, e.g., an ingot casting, and these provide the driving forces for convection within and without the mushy zone. The complexity of these flow patterns depends very much upon the configuration within a mold, on the orientation of the heat flow direction to the gravitational vector - i.e., horizontal growth, growth vertically upwards or downwards, Fig. 2. Of these geometrical alternatives, the most tractable, experimentally and analytically, is with growth vertically upwards into a positive temperature gradient, and this has received considerable attention (e.g., Sarazin et al, 1992, Bennon et al, 1987, Chen et al, 1987, Copley et al, 1970, Sample, et al 1984, Sarazin, et al, 1988). In such a case, Fig. 3, the bulk supernatant liquid, of approximately uniform composition, is thermally stabilized against convection by the positive temperature gradient. Whether or not convection takes place then depends upon the sign of the solutal coefficient of expansion, β, and whether the corresponding solutal density gradient, $\beta\ dc/dz$, exceeds the thermal density gradient, $\alpha\ dT/dz$. The system becomes unstable when the interdendritic liquid exhibits density inversion sufficiently to destabilize the quiescent, supernatant bulk liquid, i.e., when $\beta\ dc/dz > -\alpha\ dT/dz$. It is also necessary that this positive density gradient below the plane of the growth front exceed the negative gradient above by a sufficient margin to overcome the thermal and viscous inertia, and so cause a perturbation to occur. The perturbations of importance are those at or immediately above the plane of the growth front and the consequence of greatest interest in the present context is the formation of long range (e.g., $>10^2$ mm) plumes of solute-rich liquid, rising through the bulk liquid from the dendritic growth front. Such patterns have been described at length by numerous investigators, but the important aspect here is that they involve continuous re-entrainment of bulk liquid through the upper levels of the mushy zone and so offer a mechanism for sweeping out dendrite fragments into the bulk liquid, Fig. 4. In transparent systems this behavior is clearly evident and a remarkably high population density of fragments is involved, i.e., $>10\ mm^{-3}$, just above the growth front. Channel plumes of this type are observed to flow with velocities around 1 mm s^{-1} in the organic system, SCN-EtOH, up to 10 mm s^{-1} in aqueous systems, and, by extrapolation, up to ~150 mm s^{-1} in metals. With good resolution, in transparent systems, particles down to ~5 μm can be detected, and experiments are now being conducted to quantify the numbers of particles ejected from mushy zones in this way. The prospects are promising, but it should be noted that at present we are still dealing with the simplest experimental configuration and with non-metallic analogues.

(c) Particle Survival - Population Density

Again, direct measurements are possible only from transparent systems and have been or are being made at present. Simple estimates would suggest that particles around 10 μm in diameter will survive for only a few seconds at a degree or so above the liquidus temperature, so that the temperature range in which ejected fragments can be regarded as potential nuclei will be small and critical around the relevant liquidus temperature. The transition between no survivors and a shower of embryo crystals is very sharp and can be followed quite clearly as the liquid isotherms move across an analogue casting; precise temperature measurement and control are imperative in these types of experiment.

One important aspect of these studies will be to examine grain nucleation in alloys which do not, or are not expected to, exhibit thermosolutal convection. This can be done by adjusting the solutal density changes with ternary solute additions to approach an isodensity composition; this is possible for both transparent and metallic systems and is expected to reflect the presence or absence of thermosolutal transport in the grain size development under identical thermal conditions - i.e., with negligible transport there is no obvious mechanism for equiaxed grain formation by this route.

Many other ingenious, if indirect, experiments are relevant here, particularly those by Ohno (1987), who is a fervent proponent of what he calls the "separation theory," i.e., the separation of primary crystal fragments. These studies are, for the most part, only qualitative; one, for example, describes the consequences when a stainless steel filter is inserted into a molten (aluminum) alloy, which is then rapidly cooled (Fig. 5). Many equiaxed grains form above the filter, but no equiaxed crystals occur below it. Of course, although the result is striking, it does beg the main question by assuming that the nuclei were indeed detached primary fragments from the same source at an upper level, e.g., the meniscus. Another related experiment, now actually a process, shows the refining effect of mold vibration on the grain structure of continuously cast aluminum, interpreted by Ohno as resulting from crystal detachment from the mold walls, Fig. 6.

Finally, it may be remarked that in all these experimental approaches, it is most important that "clean" materials be used, clean in the sense that extraneous solids (dust, oxides, and other insolubles) be

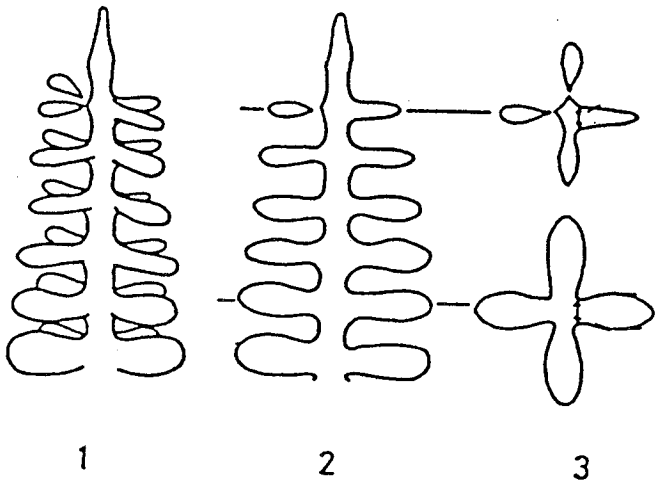

Figure 1. Schematic description of side arm separation from the primary stalk of a dendrite, Sato et al (1987).

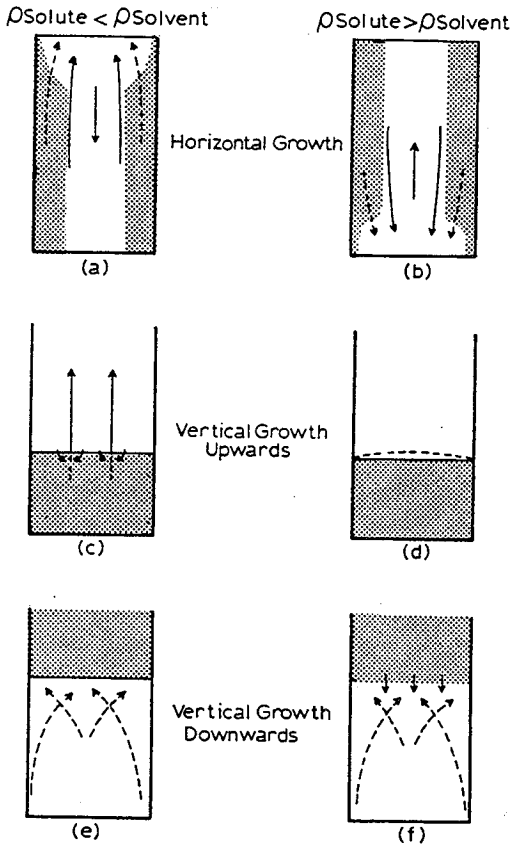

Figure 2. Alternative solidification geometries, 1-3, with schematic convection patterns for solutal density coefficient negative or positive, Sarazin et al (1988).

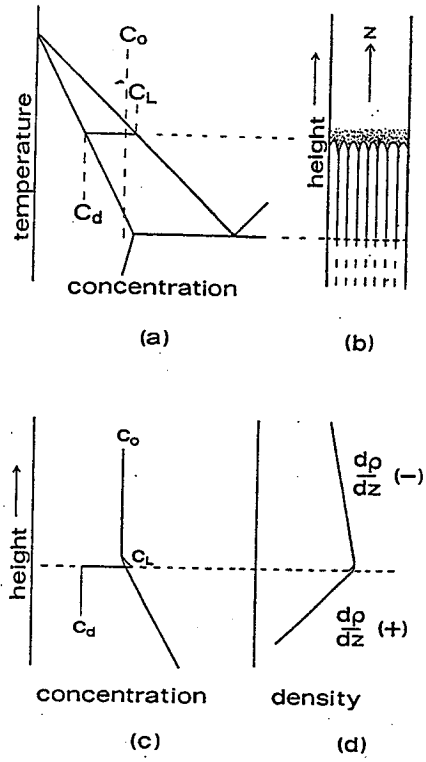

Figure 3(a-d). To show how, with a positive vertical temperature gradient and with less dense interdendritic liquid, there occurs a reversal in the vertical density gradient about the plane of a dendritic growth front, Sarazin et al (1987).

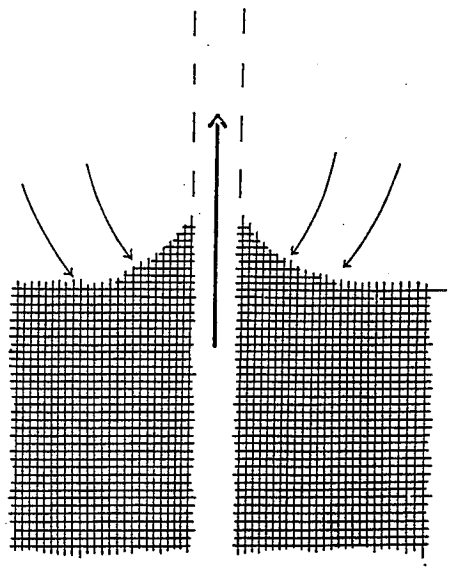

Figure 4. Mouth of segregation channel emitting solute-rich fluid in NH_4Cl-H_2O system. Schematic indicating re-entrainment pattern, Sample et al (1984).

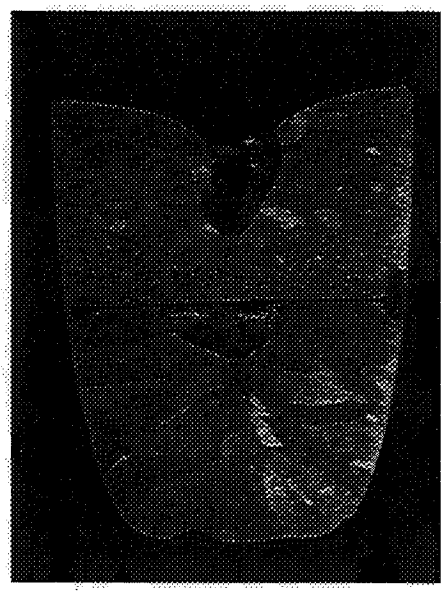

Figure 5. Showing the consequences of inserting a stainless steel filter into an aluminum melt prior to quenching; note the absence of equiaxed grains below the filter, Ohno (1987).

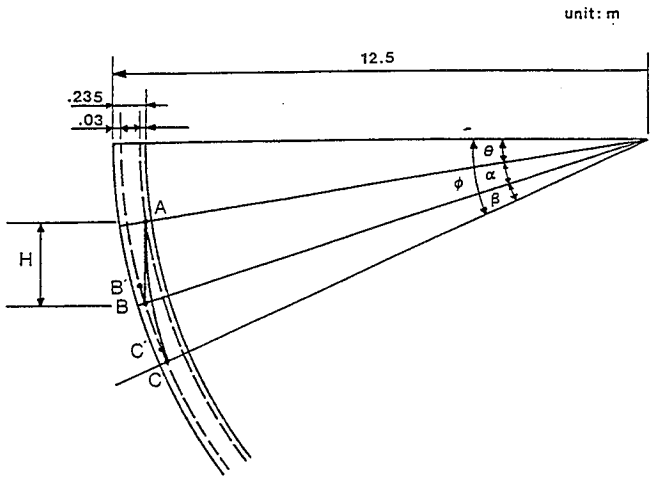

Figure 7. Schematic side view of a continuous steel caster. Crystals originating at point A fall toward point B, but, while they do so, point B moves to point C; the spatial trajectory is consequently A → C. The position of C is known. Final equiaxed grain sizes can be calculated for a range of possible positions A, i.e., a range of angles, θ, Jang et al (1991).

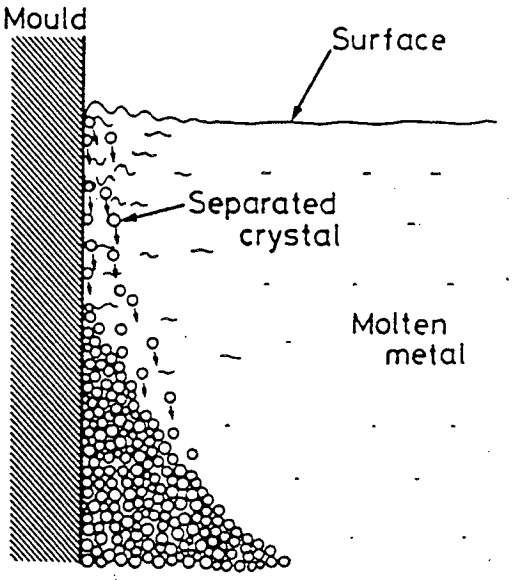

Figure 6. Depicting a mechanism for grain refining during continuous casting of aluminum caused by mold vibration, Motegi et al (1987).

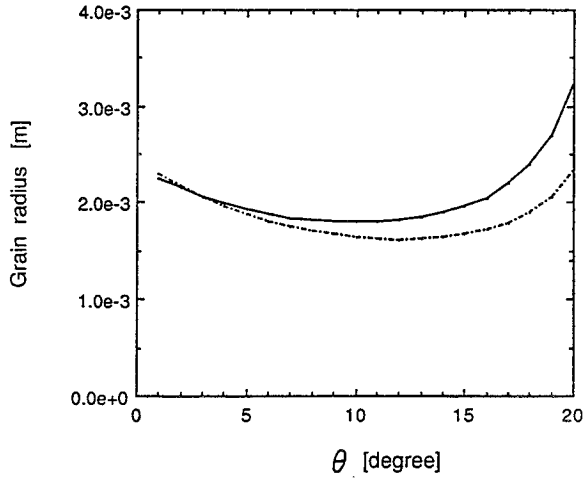

Figure 8. Necessary crystal growth rate, C_{1-i}, to cause equiaxed grains to fall from A → C, Fig. 7, over a range of origins given by θ, and the final calculated grain size, r-i, also as a function of θ, Jang et al (1991).

excluded as far as possible by filtration prior to pouring.

(d) Growth and Sedimentation

At some time and position after pouring into, or passing through, a mold, the liquid falls below the freezing point, while continuing to receive an influx of particles, in addition to any which may have survived above the liquidus. Such particles begin to grow when they fall below the equilibrium temperature for their local radii, i.e., by $\Delta T = \Gamma/r$, which will typically be of an order of 10^{-1} K. In a general case, growth will be approximately radial, but dendritic (in a eutectic cast iron, more nearly a solid sphere), so that in a cubic material the crystals are approximately octahedral in outline, generally having a small solid fraction (e.g., <5%) within an envelope of that shape. In most cases under consideration, the solid is more dense than the liquid (by <5% in metals, by ≈35% in aqueous NH_4Cl solutions), so that as crystals grow they sink and accelerate downwards as they do so. Such sedimentation has been observed and measured (Jang et al, 1991) in aqueous NH_4Cl analogue castings, and the results analyzed in terms of a simple growth law and modified Stokes' equations, i.e., modified for the small solid fraction within an assumed envelope of stagnant liquid. In this analysis it was assumed that as the crystal sinks, the surrounding liquid flows around but not through the filamentary, dendritic crystal; further discussion of the validity of such an assumption is certainly relevant to this problem (e.g., Beckerman, 1992). However, careful scaling of the physical properties in this analysis to those of a mild steel lead to an interesting correlation with the equiaxed grain size in a continuous casting. In this exercise, the geometry of a continuous slab caster was considered, Fig. 7, with information about the throughput rate (e.g., 10 mm s^{-1}) and knowledge of the position at which columnar growth on the lower, outer side became blocked by equiaxed grains—a fixed point, C. This point was identified by stopping the caster and cutting up the slab for metallographic inspection (Ishiguro et al, 1974). Point C was found to lie at ≈5 m below the upper meniscus or at an angle, $\phi \approx 24^\circ$, around the quadrant of the curved mold and casting machine. Then, working backwards from this point, it was assumed (following parallel studies of the aqueous analogue) that the relevant equiaxed grains which effected the C:E transition originated (as crystal fragments) at an unspecified position, A, close to the inner columnar growth front, at some angle θ from the horizontal meniscus at the top of the mold. Such crystal embryos as survive and grow, fall toward the lower growth front at B through a distance, H, corresponding to an angle, α. However, the casting is moving continuously, so that while the crystal was sinking (growing and accelerating) it was simultaneously translated with the slab such that point B moved to point C through an angle, β, determined by the throughput rate ($\approx 0.05^\circ\ s^{-1}$). There are some further refinements to this geometry which can be made, to include rotational aspects and to incorporate the columnar growth rate, but these are minor. Referring to position C, where $\phi = \theta + \alpha + \beta$, the physical boundary conditions are then when $\theta \rightarrow 0$ or $\beta \rightarrow 0$; i.e., the uppermost position for surviving embryos is at the upper meniscus, and the lowest position would be when A is directly above C (which, of course, is physically impossible because it would require that crystals fall with infinite speed). Within these limits it is then possible to back-calculate a range of necessary growth and sedimentation rates which would cause crystals to fall from the range of possible positions, A, to the known position, C, and, hence, over this range of θ possibilities (from $\theta = 0$ to $\theta = \phi - \beta$), a final equiaxed grain size, r_i. The results, Fig. 8, are plotted for $0 < \theta < 20^\circ < \phi = 24^\circ$, for a necessary radial crystal growth rate, C_i, to reach point C, with a final grain radius, r_i. It is found that the final grain size is remarkably insensitive to the position of origin (point A) between $\sim 5^\circ < \theta < 20^\circ$, but that an improbably large growth rate must be invoked to meet the geometrical requirements if $\theta > 15^\circ$. It was further observed that the equiaxed grain size in an actual casting was remarkably close to that so calculated, *viz.* $r_i \approx 2$ mm. This must be considered an encouraging result, but optimism must, however, be tempered by the recognition that in many alloys there are other phase transformations during subsequent cooling which may confuse correct grain size correlations with those obtained during solidification. This is particularly evident in mild steels, where there is a $\delta \rightarrow \gamma$ peritectic reaction at around 1500°C, followed by $\gamma \rightarrow \alpha$ and eutectoid reactions at lower temperatures, also compounded by possible grain growth in the γ range (over a 600 K range). Thus, in the above analysis, which would have applied to δ-iron, it was assumed that the γ grain size, following the peritectic reaction, would be in a ratio $\delta:\gamma = 1:1$. Identification of the γ grain structure is relatively easy, Fig. 9, but no assessment of γ grain growth during cooling was included in the correlation.

Some recent work by Pottore et al (1991) is particularly relevant here, in which steels of various compositions were cooled at measured rates and quenched from temperatures above, at, and below the $\delta \rightarrow \gamma$ peritectic reaction. While there is always a certain ambiguity in the interpretation of microstructures, reference to Figs. 2 or 3 of Pottore et al (1991) suggests rather convincingly that there is a close 1:1 correlation between the δ and γ grain sizes, at least in low carbon plain steels. This same paper also shows considerable γ grain growth, but the cooling rate employed, of 12 K min^{-1}, was much slower than that applicable to a continuous steel casting, where a cooling rate around 60 to 100 K min^{-1} might apply; so that in foundry practice this would be a less

important consideration and the correlation remains encouraging from a point of view of the sedimentation/growth analysis.

VISUAL OBSERVATIONS AND MEASUREMENTS

Inasmuch as the arguments and discussion presented above relate to convective transport of crystal fragments, a video record of such movements (Steube et al, 1992) can provide a more convincing demonstration than is possible with 'still' frame exposures. In presenting this paper, brief exerpts from a video-film of ammonium chloride-water castings are used to illustrate certain points. The configuration of the experiments was that of Fig. 2(c), in which solidification took place vertically upwards from a chilled copper base, in a transparent mold of square or rectangular cross section.

The warm salt solution is poured into such a mold and crystallisation of solid ammonium chloride continues for periods up to two or more hours. The optical configuration is shown schematically in Fig. 10 and employs either light or dark field illumination. Light field images of plume convection rely upon variations in refractive index with concentration and to a much smaller extent, with temperature. These are best obtained with a point light source and a translucent screen between the source and the mold. Dark field images are obtained with similar point source illumination, focused or otherwise, and depend upon light scattered from entrained crystal fragments. The latter can be used to estimate flow velocities by particle tracking or to estimate particle population densities at different levels during solidification.

Specifically illustrated in this taped record are the following:

(a) Light field illumination conveniently shows the concentration step corresponding to plume flow from a channel mouth, such as that depicted in Fig. 4. The recirculation of bulk liquid, within the upper levels of the dendritic, mushy region, causes the ejected liquid to be a little cooler (< 4 k) than its surroundings and this causes a cone of dendrites to form around the channel 'mouth'. The plume liquid is 1-2 wt.% richer in water than the surrounding and that is the cause of the refractive index difference, Fig. 11. In dark field, at the same channel mouth, fluid flow is detected by the rapid ejection of crystal fragments from the mushy region into the bulk. Simultaneously, crystal fragments can be seen to be sinking downwards onto the dendritic growth front, but with insufficient density to block this growth.

(b) Occasionally, a channel forms against the transparent mold wall and this allows more detailed inspection of movements inside the channel, below the level of the growth front. Again, referring to the schematic of Fig. 4, it may be seen how dendrite fragments separate from the inner walls of the channel. When they do so at depths down to 3-4 mm below the mouth, they are swept upwards and ejected by the recirculation pattern (Fig. 12(a)). At greater depths, (Fig. 12(b) the intra-channel liquid is essentially quiescent and such fragments slowly sink, to accumulate as polycrystalline debris at a lower level. This explains the origin of the polycrystalline structure of 'freckels' in alloy ingots.

(c) Finally, the 'open' supernatant, bulk liquid may be illuminated by a divergent laser beam to provide a band (e.g. ~ 1 mm deep) of light at some height above the growth front. Observation of this band from an angle above or below the plane, e.g. at 45 , then allows an estimate of the planar particle density to be made from scintillations as the crystal fragments pass through that plane, Fig. 13. The positions of convection plumes can readily be detected from such records by the local presence of more frequent, brief scintillations.

CONCLUSIONS

In summary, the following points are made:

(i) There is an alternative modeling route to describe grain nucleation from a melt which should be more physically realistic in many cases than one based on an assumption of heterogeneous nucleation on indeterminate substrate particles. This model identifies the nucleating particles as being fragments of the base material itself, inherently introduced into the system during pouring and solidification.

(ii) It is feasible to describe this nucleation process by four interrelated steps involving (a) the generation of fragments, (b) the transport of these into bulk liquid, (c) the survival of such crystal fragments, and (d) the growth and settling of the resulting grains.

(iii) Experimental and analytical approaches have been briefly reviewed with reference to each of these four steps. It was noted that the experimental studies must rely heavily on the use of transparent organic or aqueous analogues for metallic castings and necessarily require careful scaling of the physical properties to warrant extrapolation of analyses to metals.

(iv) It is claimed that this alternative approach is more physically correct than that currently used, and, as such, could have a predictive capability which is presently lacking. It must be admitted, however, as a cautionary comment, that it may be difficult to formulate some of these steps with

sufficient confidence. If this cannot be achieved, it may be that attempts to model the global solidification process will remain physically flawed and therefore be of limited predictive potential. Notwithstanding, current efforts are promising.

ACKNOWLEDGEMENTS

This presentation follows recent studies of the effects of natural convection on segregation during solidification, supported by the National Science Foundation, Division of Materials Research, Grant #DMR88-15049, and NASA, Microgravity Science and Applications Office, through Lewis Research Center, Grant #NAG-3-560.

REFERENCES

Avrami, M. 1939, J. Chem. Phys., 7, 1103, et seq., 1940 and 1941.

Beckermann, C., 1992, Nature and Properties of Semi-Solid Materials, TMS Spring Meeting, San Diego, CA, to be published.

Bennon, W. D. and Incropera, F. P., 1987, J. Heat and Mass Transfer, 30, 2161-2170.

Biloni, H. and Chalmers, B., 1968, J. Mat. Sci., 3, 139.

Bommaraju, R., Brimacombe, J. K. and Samarasekera, I. V., 1984, Trans. I.S.S., 5, 96.

Bower, T. F. and Flemings, M. C., 1967, Trans. AIME, 239, 1620.

Chalmers, B., 1963, J. Australian Inst. Metals, 8, 225.

Chen, C. F., Briggs, D. G. and Wirtz, R. A., 1971, J. Heat and Mass Transfer, 14, 57-65.

Copley, S. M., Giameik, A. F., Johnson, S. M. and Hornbecker, S. M., 1970, Metall. Trans., 1A, 2193-2204.

Davies, G. J., 1973, *Solidification and Casting*, Chapter 6, Applied Science Publishing Co., London.

See, e.g., Engineering Foundation Conference Proceedings on the Modeling of Castings and Welding Processes, I-V, 1980-1991; Solidification Processing 1987, Institute of Metals, Book #421; TMS Publications: Computer Simulation of Microstructural Evolution, 1986, and Casting of Near Net Shape Products, 1988.

Genders, R., 1926, J. Inst. Metals, 35, 259.

Glasson, E. L. and Emley, E. F., 1967, *The Solidification of Metals*, The Iron and Steel Institute, Book #110, 1-9.

Glicksman, M. E. and Schaefer, R. J., 1968, *The Solidification of Metals*, Iron and Steel Inst. Book #110, 43-48.

Goettsch, D. D. and Dantzig, J. A., 1992, Nature and Properties of Semi-Solid Materials, TMS Proceedings, 159-199.

Hellawell, A., 1979, *The Solidification and Casting of Metals*, The Metals Society Publication #192, 161-168.

Hellawell, A., Sarazin, J. R. and Steube, R. S., to be published.

Hoffmeyer, M. K. and Perepezko, J. H.,1989, Scripta Met., 23, 315-320.

Glicksman, M. E. and Voorhees, P. W., 1984, Metall. Trans., 15A, 995.

Glicksman, M. E., Marsh, S. P., Smith, R. N. and Kuklinski, R., 1992, Nature and Properties of Semi-Solid Materials, TMS Proceedings, 19-39.

Ishiguro, M., Kawakami, K., Ito, M. and Miyoshi, S., 1974, J. Japan Iron and Steel Inst., 60, 147-155.

Jackson, K. A., Hunt, J. D., Uhlmann, D. R. and Seward, T. P., 1966, TMS-AIME, 236, 149-160.

Jang, J. and Hellawell, A., 1991, J. Ironmaking and Steelmaking, 18(4), Parts I and II, 267-274 and 275-284.

Kattamis, T. Z. and Flemings, M. C., 1965, TMS-AIME, 233, 992.

Kattamis, T. Z., Coughlin, J. and Flemings, M. C., 1967, TMS-AIME, 239, 1504.

Lait, J. E, Brimacombe, J. K. and Weinberg, F., 1974, J. Ironmaking and Steelmaking, 1, 35.

Maxwell, I. and Hellawell, A., 1975, Acta Met., 23, 239-249.

Motegi, T. and Ohno, A., 1987, *Solidification Processing*, Inst. of Metals, Book #421, 176-179.

Ohno, A., *Solidification: The Separation Theory and Its Practical Applications*, Springer-Verlag, 1987.

Oldfield, W., 1960, BCIRA Journal, 8, 177-192.

Oldfield, W. 1966, Trans. ASM, 59, 945-958.

Pottore, S. N., Garcia, C. I. and DeArdo, A. J., 1991, Metall. Trans., 22A, 1871-1880.

Rappaz, M., 1989, Int. Materials Reviews, 34, 93-123.

Rosenhain, R., 1926, J. Inst. Metals, 35, 282.

Sample, A. K. and Hellawell, A., 1984, Metall. Trans. 15A, 2163-2173.

Sarazin, J. R. and Hellawell, A., 1988, Metall. Trans., 19A, 1861-1871.

Sarazin, J. R., Steube, R. S. and Hellawell, A., 1992, Nature and Properties of Semi-Solid Materials, TMS Proceedings, 143-152.

Sato, T., Kurz, W. and Ikawa, K., 1987, Trans. Japan Inst. Metals, 28, 1012- 1021.

Southin, R. T., 1967, TMS-AIME, 239, 220.

Stefanescu, D. M. and Chandrashekhar Kanetka, 1986, Computer Simulation of Microstructural Evolution, TMS Proceedings, 171-188.

Stefanescu, D. M. and Rappaz, M., 1988, Solidification Processing of Eutectic Alloys, TMS Proceedings, 133-151.

Steube, R. S. and Hellawell, A., Int. Video Journal of Engr. Research, to be published.

Thevoz, Ph., DesBoilles, J. S. and Rappaz, M., 1989, Metall. Trans., 20A, 311-322.

Voorhees, P. W. and Glicksman, M. E., 1985, J. Crystal Growth, 72, 559.

Voorhees, P. W., 1990, Metall. Trans., 21A, 27-37.

(a)

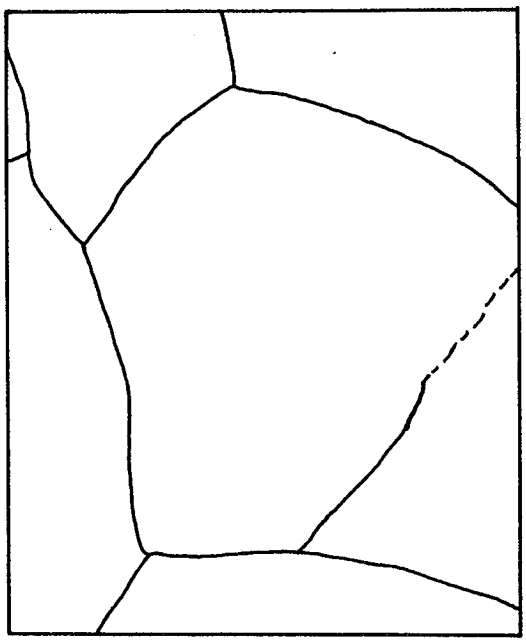

(b)

Figure 9(a)(b). Identification of γ grain structure in a 0.2 wt.% carbon plain steel casting, following ferrite precipitation and the pearlite transformation, Jang et al (1991).

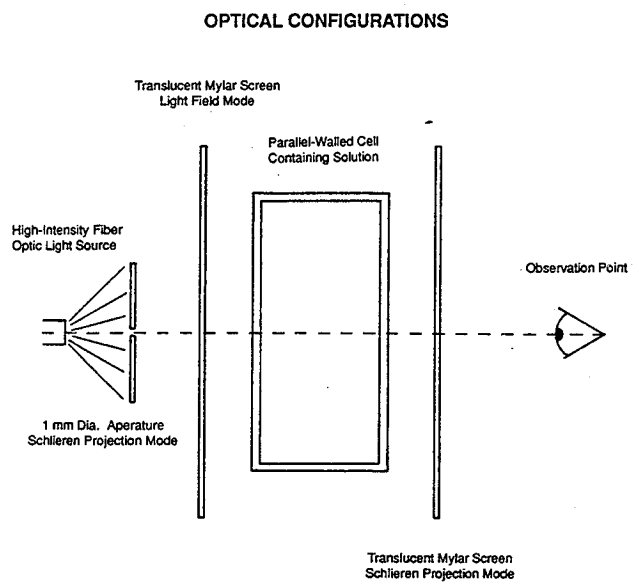

Figure 10. Optical configurations for observation of convection patterns in transparent analogue castings.

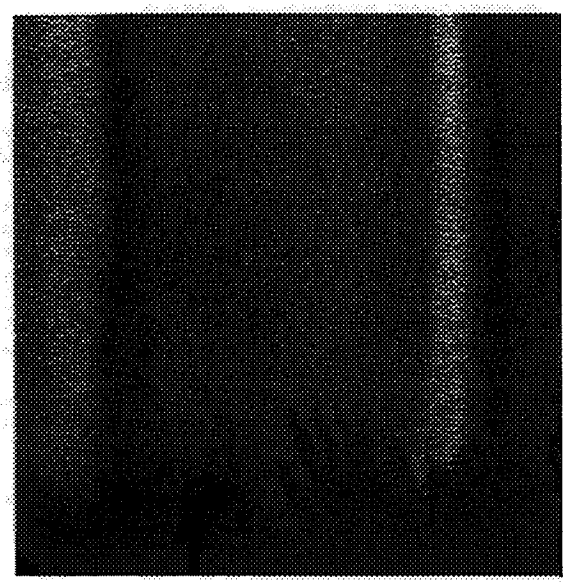

Figure 11. Light field image of solute plume flowing out of channel mouth in NH_4Cl-70 wt.% water casting. Plume width > 1 mm.

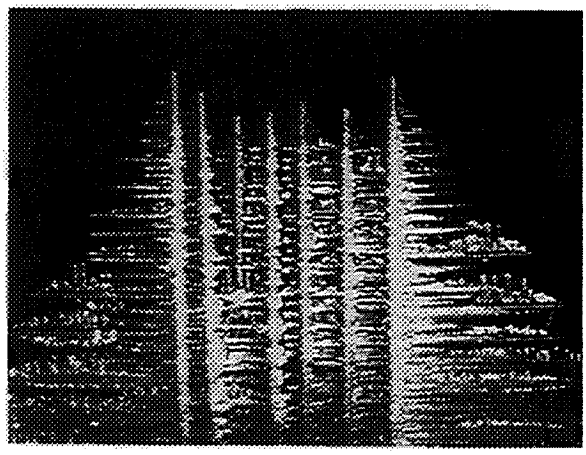

(a)

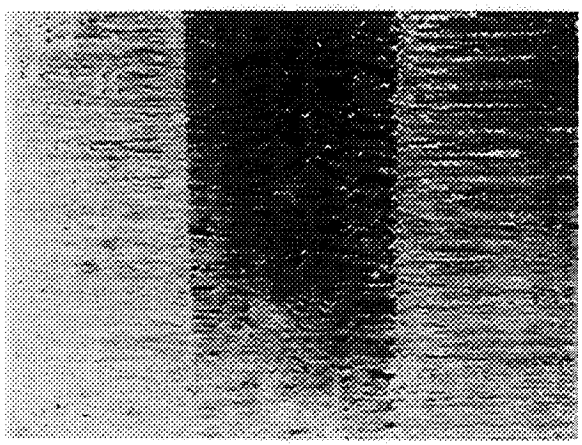

(b)

Figure 12(a). View of channel mouth at mold wall and (b), approximately 3 mm lower, where dendritic fragments begin to collect as debris. Channel width > 1 mm.

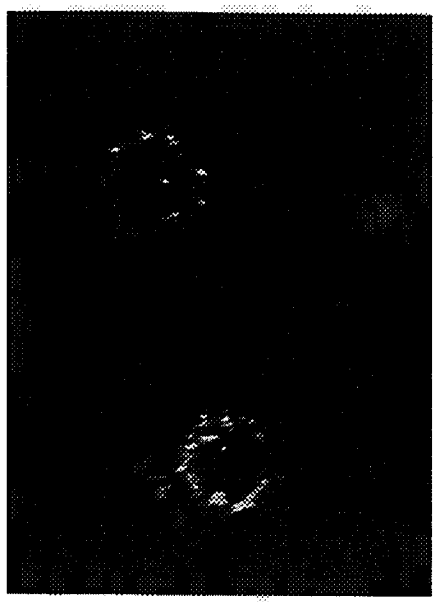

Figure 13. Top view dark field image of illuminated plane, 0.5 mm deep, using HeNe Laser. Plane approximately 4 mm above growth front, showing particles entrained in channel plumes. The position of channel mouths are distinguishable.